

Improvement of Phase Unwrapping Algorithms by Epipolar Constraints

Johannes Köhler, Jan C. Peters, Tobias Nöll and Didier Stricker

German Research Center for Artificial Intelligence, Trippstadter Str. 122, 67663 Kaiserslautern, Germany

Keywords: Structured Light, Fringe Projection, Phase Shifting, Phase Unwrapping.

Abstract: Phase unwrapping remains a challenging problem in the context of fast 3D reconstruction based on structured light, in particular for objects with complex geometry. In this paper we suggest to support phase unwrapping algorithms by additional constraints induced by the scanning setup. This is possible when at least two cameras are used, a likely case in practice. The constraints are generalized for two or more cameras by introducing the concept of a candidate map. We claim that this greatly reduces the complexity for *any* subsequent unwrapping algorithm, their performance is thereby strongly increased. We demonstrate this by exemplarily integrating the candidate map into a local path following and a global minimum norm unwrapping method.

1 INTRODUCTION

Phase shifted structured light is a well known and widely used method in the field of 3D reconstruction. In this technique, a linear phase function is encoded by shifted sine waves and the resulting fringe patterns are projected onto an object. If these projections are recorded by a camera, the corresponding phase values can be recovered from the captured images. The resulting phase images induce pixel-wise correspondences of very high quality among all involved devices. These correspondences then can be used for depth recovery. One of the biggest advantages of phase shifting is its robustness towards the projector's narrow depth of field. The projected sinusoidal fringe patterns can still be robustly decoded even if they are out of the projector's focus range.

However, the desired phase function can only be recovered modulo- 2π . This is an inevitable consequence of the involved trigonometric functions, whose inverse functions are always restricted to the principal branch. *Phase unwrapping* denotes the resolution of these ambiguities (Figure 1).

Although this problem has been studied for decades (Gorthi and Rastogi, 2010), a fully robust and reliable solution has yet to be found for a single frequency level. A successful unwrapping heavily depends on the object scanned and is particularly difficult near depth discontinuities. Most everyday objects are not convex, depth maps of the corresponding object consequently will contain such discontinuities (Figure 2 (a)). Perspective projection causes unrelated

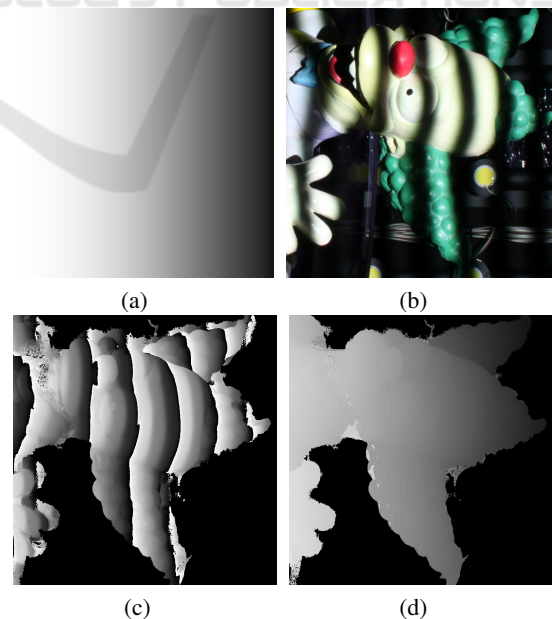


Figure 1: Individual steps for transmitting a phase from the projector to a camera. (a) The projector's phase before sinusoidal encoding into a fringe pattern. (b) Projected fringe pattern. (c) Wrapped phase recovered from multiple fringe patterns captured by a camera. (d) Unwrapped phase.

phase intervals to seamlessly blend into each other at such regions, which poses a great challenge to phase unwrapping algorithms (Figure 2 (b)). The transition can be more or less smooth, which is very hard to detect.

In this paper we follow the recent trend to uti-

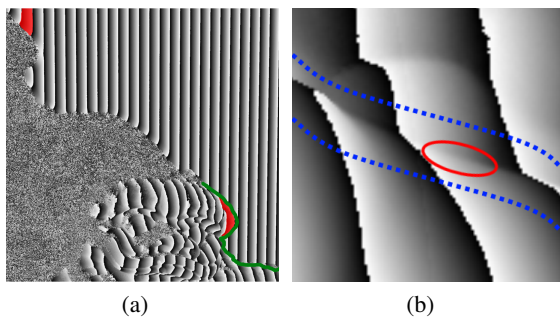


Figure 2: (a) Prominent foreground/background discontinuity (the green line separates foreground (object) and background (wall)). Two exemplary parts that belong to the same wrap count (i.e. to the same stripe) are colored red. (b) Stripes with different wrap counts seamlessly blending into each other (red) at a depth discontinuity (enclosed by blue lines).

lize the geometry of multiple cameras for unwrapping (Bräuer-Burchardt et al., 2008; Bräuer-Burchardt et al., 2011; Bräuer-Burchardt et al., 2013; Garcia and Zakhor, 2012). In these publications, the epipolar geometry of two cameras was used to constrain the potential unwrapping possibilities. However, the epipolar geometry alone is not sufficient for unwrapping, many ambiguities remain and further steps are necessary. In this paper, we propose a more general approach to use the epipolar geometry. We generalize its use to more than two cameras and introduce the *candidate map*, which stores all geometrically feasible unwrapping possibilities for a single camera. In contrast to state of the art methods, we do not focus on a single method to resolve the remaining ambiguities. Instead, we suggest to use the candidate map as an appropriate support for *any* classic phase unwrapping algorithm. The candidate map can drastically improve their performance, we demonstrate this by including it into two exemplary state of the art unwrapping methods.

2 RELATED WORK

Existing phase unwrapping approaches can be roughly grouped into temporal and spatial methods. Temporal methods use additional patterns to remove the ambiguity. All temporal methods have in common, that the additional patterns encode the period of the desired phase. (Wang et al., 2010) proposes sinusoidal patterns with different frequencies for this. The method starts with a phase function whose encoding yields no wrapping but poor phase quality. The frequency is consecutively increased while the wrapping is resolved using the previous levels. With the

correct frequency gain, this method yields correctly unwrapped phases even for objects with many discontinuities and has the same advantages than phase shifting itself. Other authors propose binary codes for this task (Bergmann, 1995). Temporal methods are fully local, i.e. the unwrapping decision for a single pixel does not depend on his neighbors and are thus robust even for complex objects with many depth discontinuities. However, they require a large amount of additional images to be captured, which might not be possible in application domains such as real time scanning.

Spatial methods require less projected patterns and try to unwrap the phase using neighborhood information. Existing spatial approaches can be roughly grouped into two categories: Path following and minimum norm.

Path following methods (Goldstein et al., 1988; Herráez et al., 2002; Abdul-Rahman et al., 2007; Lof-feld et al., 2008; Martinez-Espla et al., 2009) start at a given pixel and unwrap the phase along a path in the image by adding or subtracting multiples of 2π to the current pixel's phase value. The path to follow can be fixed or dynamically guided by a phase quality measure. Algorithms of this kind are also called *local* methods, since at every step they just inspect pixels near the current position.

In contrast to this, minimum norm methods (Ghiglia and Romero, 1996; Costantini, 1998; Dias and Leito, 2002; Bioucas-Dias and Valado, 2007) globally minimize an unwrapping cost function defined for each pair of neighboring pixels. Both approaches suffer from inaccuracies at depth discontinuities, where unrelated phase intervals can seamlessly blend into each other (Figure 2).

The aforementioned methods are purely image based and rely on a single viewpoint. Several authors recently proposed to use two viewpoints and their corresponding epipolar geometry for phase unwrapping. This allows to deduce local (i.e. pixelwise) constraints. Common to all methods is the fact, that epipolar constraints alone are not sufficient for a correct unwrapping, many ambiguities remain. It is thus important to apply additional steps for computing the desired phase. (Bräuer-Burchardt et al., 2008) were the first to use epipolar geometry. They use a disparity map to resolve the remaining ambiguities, which is also related to the epipolar geometry. In their follow up paper (Bräuer-Burchardt et al., 2011), they use combinatorial considerations, but unwrapping ambiguities can still remain. (Bräuer-Burchardt et al., 2013) tries to resolve the ambiguities with a special hardware and parameter arrangement. However, this reduces the generality of the hardware setup, these restrictions

might thus not be admissible in every scenario. (Garcia and Zakhor, 2012) also use a stereo camera setup and propose two approaches to resolve the remaining ambiguities. The temporal approach is not relevant in our context, as we focus on static scene reconstruction. The energy minimization approach can be considered as special case of our proposed framework.

In contrast to state of the art methods, which usually use only two cameras, we generalize the use of epipolar geometry to n cameras by introducing the *candidate map* in this paper. The candidate map does not unambiguously unwrap the phase, but it strongly constrains the available possibilities. We believe that existing unwrapping methods can be used to achieve this and thus suggest to use the candidate map as reasonable preprocessing step for *any* classical phase unwrapping method.

3 PHASE GENERATION

In the context of this paper, phases are generated with phase shifted structured light. A phase is thus defined in the image plane of a projector as a linear function $\Phi(x, y) \in [0..2\pi N]$ (Figure 1 (a)). Φ can be projected onto an object and recovered from the point of view of a camera by encoding it with a sine or cosine function and shifting it K times. This results in shifted fringe patterns captured in K camera images, an exemplary camera image with a pattern projected onto an object is illustrated in Figure 1 (b). For each pixel it is then possible to compute $\tan(\phi)$ using e.g. (Guo et al., 2007), where ϕ is the desired object phase seen from the respective camera. The tangent results from the periodicity of the involved trigonometric functions and the inverse tangent thus does not yield ϕ , but the wrapped object phase $\psi = \phi \bmod 2\pi$ (Figure 1 (b)). Note that the parameter N defines the amount of periods and thus also the wrap count of ϕ .

Without loss of generality, we restrict Φ to have a constant gradient $\nabla\Phi = d$, $d \in \mathbb{R}^2$. This simply constrains the isocurves of Φ to be straight lines, as opposed to e.g. (Peng and Gupta, 2008). For $d = (1, 0)$, Φ would thus correspond to e.g. Figure 1 (a) and we would project vertical fringes. We use this property in Section 4 to relate the phase to the camera geometry.

4 CANDIDATE MAP GENERATION

Depth reconstruction based on structured light can be accomplished with a video projector and a single

camera. If more cameras are present, they naturally restrict the unwrapping possibilities. In practice it is likely to have more than one camera, because triangulation with only cameras does not require a gamma calibration (Guo et al., 2004) in contrast to triangulation with a camera and the projector (Han and Huang, 2009).

In the following, we consider a scanning setup with one projector and $n \geq 2$ cameras and derive phase constraints from the devices' epipolar geometry. Our method requires only the fundamental matrix, it is thus not stringently required to fully calibrate the cameras by estimating their poses and intrinsic parameters (focal length, principal point and distortion coefficients). However, a structured light scanner is usually calibrated and especially a prior calibration of the camera's distortion coefficients and undistortion of the respective images greatly improves the accuracy of the method. For an uncalibrated setup, the fundamental matrix is easily computed from 2D correspondences (Hartley and Zisserman, 2004).

The method sketched in Section 3 yields a wrapped object phase ψ_i for each camera (Figure 1 (c)). For every wrapped phase value $\psi_i(x, y) \in [0..2\pi]$ there is exactly one $w \in \{0..N-1\}$ such that $\psi_i(x, y) + w \cdot 2\pi = \phi_i(x, y)$. w is the desired period or, in other words, the index of the correct stripe (Figure 1 (c)). It adds the multiple of 2π required for unwrapping and we consider it as the wrap count.

The task of *each* unwrapping algorithm thus is to find the correct w for each pixel of ψ_i . To formally handle all possible values of w , we define the *candidate map* C_i :

$$C_i : \mathbb{N}^2 \rightarrow \mathcal{P}\{0, \dots, N-1\} \quad (1)$$

where \mathcal{P} is the power set operator. For each pixel of a primary view there are N unwrapping possibilities and the candidate map stores a subset of geometrically feasible wrap counts for each pixel: $C_i(x, y) \subseteq \{0, \dots, N-1\}$.

C_i is called *consistent* at position (x, y) , if the correct wrap count w is present in $C_i(x, y)$. Pixels (x, y) with $|C_i(x, y)| = 1$ are called *singletons*. If a singleton is consistent, it correctly unwraps the phase without ambiguities.

Since the correct unwrapping must be consistent among the devices, secondary views can drastically reduce the feasible amount of unwrapping possibilities $|C_i(x, y)|$ (Figure 3).

In the following we compute a candidate map C_i by enforcing epipolar phase consistency among multiple secondary views. Given $n \geq 2$ views, a primary view i , fundamental matrices F_{ij} from the primary view i to each secondary view j , F_{ip} from the primary view i to the projector and F_{pj} from the projector to

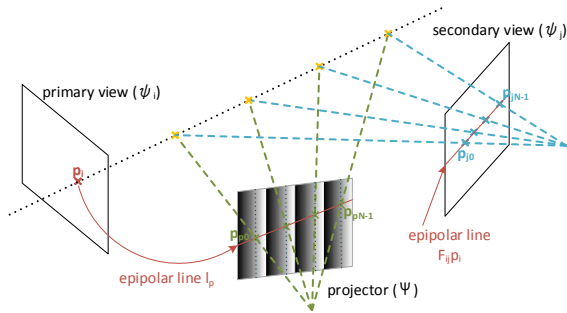


Figure 3: Geometry of all unwrapping candidates for $N = 4$. If $|\Psi_i(p_i) - \Psi_j(p_{j_k})| > \epsilon$, the corresponding candidate can be excluded *before* an unwrapping algorithm is applied (zoom in for details). At the dotted lines, $\Psi = \Psi_i(p_i)$.

each secondary view, we can restrict the unwrapping candidates $C_i(p_i)$ for each primary view pixel p_i by applying the following steps:

- Compute epipolar line $l_p = F_{ip}(p_i, 1)^T$ in the projector image plane. The periods of the projector's phase touched by this line are relevant for unwrapping. In Figure 3, all 4 exemplary periods are thus relevant.
- Compute intersections $p_{p_0} \dots p_{p_{N-1}}$ of l_p with each phase isoline corresponding to $\phi_i(p_i)$. These are the projector pixels with a phase value of $\phi_i(p_i)$ that could have illuminated p_i .
- Each of these intersections defines a unique point in a secondary view: We propagate the phase line intersection points p_{p_k} to each secondary view j by computing the intersection points p_{j_k} of the epipolar line pairs $(F_{ij}(p_i, 1)^T, F_{pj}(p_{p_k}, 1)^T)$. The resulting pixels potentially perceive the same object point and thus should have the same phase value than the primary view $(\Psi_i(p_i))$.
- if $|\Psi_i(p_i) - \Psi_j(p_{j_k})| < \epsilon$, it can be assumed, that the secondary view j perceives the same wrapped phase value. Due to occlusions, this will not hold for all secondary views. We thus add the corresponding wrap count to $C_i(x, y)$, if this condition holds for $m \leq n - 1$ secondary views, which means that m secondary views agree on the perceived phase value.

Remark: It is required for numerical stability, that the angle enclosed by a phase line and an epipolar line is not too low. As a rule of thumb for two cameras and a projector setup, the devices should be placed on a straight line that has $\nabla\Phi$ as directional vector. E.g. for cameras placed on a table to the left and right of a projector such that the image planes are parallel, the epipolar lines are parallel to the image planes' x-axis. A phase with $\nabla\Phi = (1, 0)$ would then be optimal, as

the phase's isolines and the epipolar lines are perpendicular.

5 PHASE UNWRAPPING

In general, the performance of most phase unwrapping algorithms can be greatly enhanced by augmenting them with a candidate map. This does not only reduce the amount of unwrapping possibilities per pixel but can also directly constrain the starting pixels to the correct phase value. This is in fact a serious disadvantage shared by many unwrapping methods: The unwrapped phase produced by the respective algorithm might be consistent in itself but shifted with respect to the original phase projected onto the object. This is caused by the fact that a wrap count w needs to be assigned to the starting pixels for initialization. Subsequent pixels are unwrapped relative to this w . Since an initial w cannot be correctly determined without additional information it must later be corrected, which might not always be possible. The singletons of the candidate map, which are unwrapped correctly, implicitly solve this problem. In the following, we sketch how to integrate the candidate map into a local path following algorithm and outline a new global minimum norm algorithm based on graph labeling.

5.1 Local Unwrapping by Region Growing

As an exemplary local unwrapping algorithm we choose the region growing method of (Xu and Cumming, 1999). This algorithm starts growing regions from multiple pixels of high data quality and propagates the phase along paths with high unwrapping confidence. A pixel p is unwrapped using a weighted mean of predictions based on extrapolations of neighbouring pixels that are already unwrapped in a 5×5 window centered at p . The process is illustrated in Figure 4. Predictions are made following K straight lines originating from p . If in a direction k there is only one unwrapped pixel, the corresponding prediction is constant and the associated weight is set to 0.5. In case there are two already unwrapped pixels along the prediction line, a linear extrapolation is used and $w_k = 1$ since these predictions are more reliable than the constant ones. Then a composite prediction $\tilde{\phi}(p)$ is formed as weighted average of the individual predictions. This composite prediction is used in an unwrapping attempt for p :

$$\phi(p) = \Psi(p) + 2\pi s \quad \text{with} \quad s = \left\lceil \frac{\tilde{\phi}(p) - \Psi(p)}{2\pi} \right\rceil \quad (2)$$

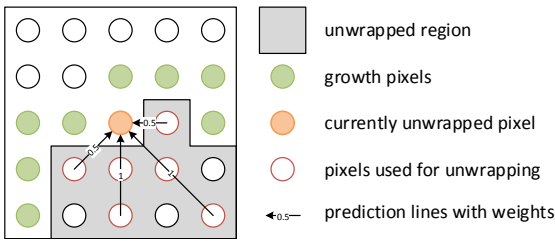


Figure 4: Unwrapping by region growing and phase prediction. This figure is based on an illustration in the original paper (Xu and Cumming, 1999).

The operator $[\cdot]$ denotes rounding to the nearest integer. The essence of this approach is the same as for the level based temporal unwrapping, note the striking similarity of Equation 2 and Equation 7 of (Wang et al., 2010). However, the wrap count in our case is estimated from the neighborhood instead from additional patterns. The unwrapping is accepted after additional reliability checks, please refer to the original paper for more details.

Although the method starts from multiple local positions, we found that it cannot fully cope with discontinuities where the phase values with different wrap counts seamlessly blend into each other (Figure 1 (d)). Integration of the candidate map can resolve this and is straightforward: We start growing regions only from singletons, the phase is thus directly unwrapped without having to deal with the relative shift problem. In addition to the original reliability checks, we allow an unwrapping at p only, if the corresponding wrap count is found in the candidate map. In our evaluation we show that this greatly stabilizes the unwrapping process.

5.2 Global Unwrapping by Graph Labeling

The application of graph cut based optimization to labeling problems had a large impact on image processing during the last decade (Kolmogorov and Zabini, 2004; Boykov et al., 2001). Given an undirected graph $G = (V, E)$ and a set of labels $L = \{l_1, \dots, l_N\}$, a (graph) labeling of G is a mapping $\ell : V \rightarrow L$. Furthermore there are weights placed on vertices and edges of the graph. First order weighting functions are defined for the vertices and depend on the label of the respective vertex. Second order weighting functions are defined for each edge, they depend on the weights of the associated vertices. The ultimate goal then is to compute a labeling of the graph that minimizes the sum of all weights.

The graph labeling technique was also used for phase unwrapping (Bioucas-Dias and Valado, 2007).

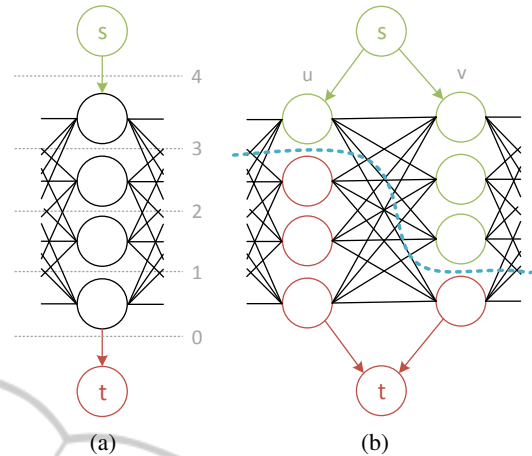


Figure 5: Parts of the graph G' for $N = 5$. Left: Representatives of a single pixel from G . The dashed lines illustrate the possible cuts and the associated wrap-counts. Right: Representatives of two pixels u, v and their connections. The blue dashed line is a possible graph-cut, the vertices are colored according to the side of the cut they are on.

It relates to unwrapping in the following way: Each pixel yields a vertex and neighboring pixels are connected by an edge which results in a graph G . Each $w \in \{0..N-1\}$ represents a label and each pixel of a wrapped phase is unwrapped by labeling it with one w . The costs for a certain labeling are defined only by second order weighting functions for each pair of neighboring pixels. Minimization can then be accomplished using a graph cut. Since graph cuts optimize binary labeling problems however, we follow the “k to 2” method of (Schlesinger and Flach, 2006) to transform our N -ary labeling problem to a binary one. In the corresponding new graph G' , each vertex (i.e. each pixel) of the old one is represented by $N-1$ vertices. Where there is an edge (u, v) in G , the representatives of u and v are fully interconnected in G' . Moreover, there are two special vertices s and t in G' which provide the source and sink for the graph-cut calculation and are connected to the first and last representatives of each pixel, respectively. The spaces between representatives themselves and between them and s and t stand for the labels or here wrap-counts which are identified with possible graph-cuts in G' . The situation is illustrated in Fig. 5.

Our cost function for the edges is

$$f(p_0, p_1, w_0, w_1) = \|2\pi w_0 + \psi(p_0) - (2\pi w_1 + \psi(p_1))\| \quad (3)$$

for a wrapped phase ψ , pixels p_0 and p_1 and wrap counts w_0 and w_1 . This function in particular penalizes unwrapping over discontinuities, where $|w_0 - w_1| > 1$.

After computing a min-cut on G' the wrap-count for each pixel is determined by assigning each repre-



Figure 6: The two objects used for evaluation. “Krusty” is a gum figure with smooth geometry, it yields rather smooth phases. The “Allegorie” is mostly made from metal and marble, it yields rather noisy phases. Moreover, its highly non-convex nature yields many self-occlusions. The respective discontinuities make the phases very hard to unwrap.

sentative the side of the cut it is on and by finding the gap with the transition from source to sink, as indicated in Figure 5. However, the sheer size of the graph results in high memory consumption and high computation time. Especially for high camera resolutions, the computation of a min-cut becomes intractable.

The advantage of this method is the straightforward application of the candidate map: The structure of the candidate map is directly reflected in the graph and all geometrically unfeasible labelings can be omitted. This relaxes the problems mentioned above: The number of representatives for each pixel and thus the memory consumption is drastically reduced, which also speeds up the process considerably. Similar to the region growing approach, singletons fix the relative shift problem in this context, too. In our evaluation, we apply the method to 15 megapixel phase images, which is not possible without the candidate map.

6 RESULTS

To prove the validity of the suggested methods, we apply them to scans of two objects with very different texture and geometric complexity (Figure 6). The first object (“Krusty”) is a figurine made of gum. Its coloring is simple, every region features one hue. The object geometry is also quite simple, there are only few

rough edges and the surface is mostly smooth. From most viewpoints, it yields phases with low noise, that are rarely disrupted by discontinuities. The second object (“Allegorie”) is a statue made from different materials, mostly brass and marble. These materials produce a phase with more noise. The complex geometry causes many self-occlusions and depth discontinuities from most view points, which makes the phase significantly harder to unwrap.

Both objects were scanned with multi-frequency phase shifting with a setup of one Sanyo[®] Z 4100 projector (1920x1080) and seven Canon[®] EOS[®] 500D cameras (4752x3168). We used five frequency levels $N = \{1, 5, 11, 27, 91\}$ with three shifts for the first four levels and ten shifts for the fifth level for better noise reduction. With these parameters, the multi-frequency unwrapping algorithm of (Wang et al., 2010) is able to correctly unwrap each level, we thus use this phase as ground truth. Note that this unwrapping algorithm requires substantially more input images due to the additional levels, which is intractable in some application domains such as real time scanning. In all experiments, the amount of required secondary views (m) is two.

Figure 7 (top row) shows the candidate maps and the results of the proposed unwrapping algorithms for $N = 27$ and $N = 91$. For both objects, large parts of the candidate maps are filled with singletons. As one would expect, the amount of candidates is larger for $N = 91$. The second row of Figure 7 shows the results of the region growing algorithm without candidate map. Since the algorithm does not know the correct phase period at its starting pixels, it assigns a fixed w . Regions blending into each other are then merged, i.e. the wrap count of one unwrapped region is shifted to be consistent with the other region. However, consistent merging is not possible anymore as soon as an unwrapping path crosses a depth discontinuity that has a smooth phase (Figure 1 (d)). This causes multiple self-consistent patches, whose phase is shifted (unicolored, non-green regions). An augmentation of this algorithm with the candidate map almost fully resolves this problem (Figure 7, third row). This is a remarkable result, in particular for the “Allegorie” dataset, whose complex geometry with many depth discontinuities yield phases that are very hard to unwrap. Since the unwrapping is restricted to $|C_i(p)| > 0$ however, the unwrapped regions are smaller for both objects. This could be improved by applying classic approaches to regions with $|C_i(p)| = 0$ after unwrapping with the candidate map, if the corresponding region is connected to an unwrapped part. At $N = 91$, the performance of the augmented algorithms is worse than at $N = 27$, but still better than

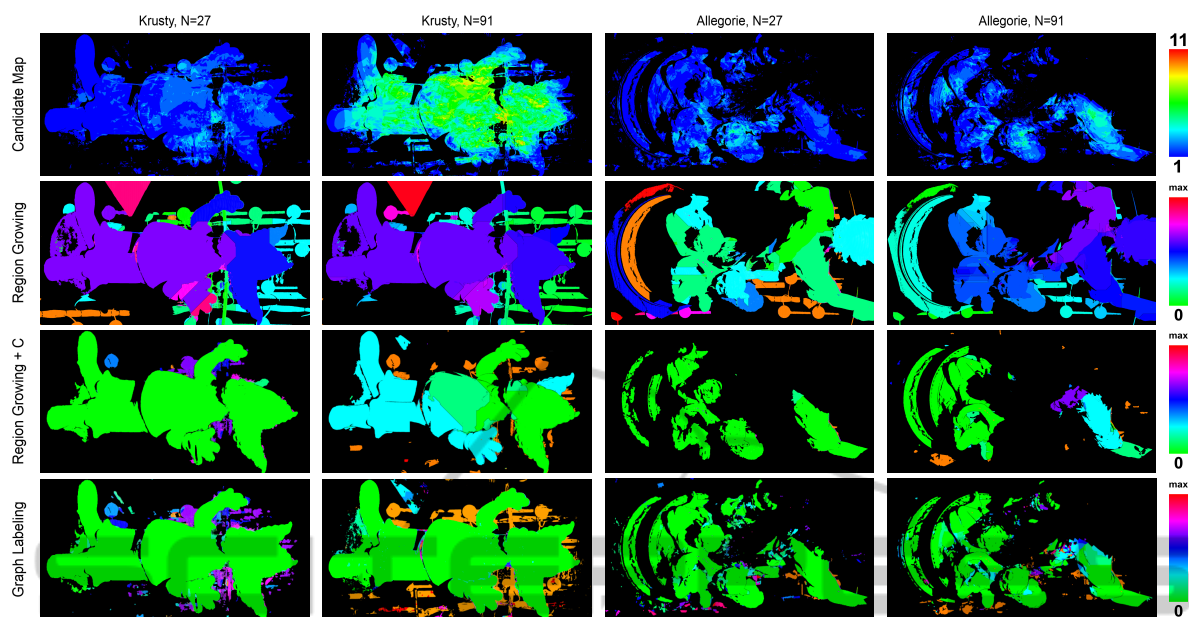


Figure 7: Candidate maps and results of the enhanced unwrapping algorithms. For the unwrapping results (row 2-4) we visualize the period difference to the reference phase. Green corresponds to correct unwrapping, red to the highest measured difference for this dataset. Everything but green yields wrong depth values.

without the candidate map. In case of the gum figure, this is caused by the presence of only few singletons, that are distributed along the border. In this region, the surface normal is almost orthogonal to the view direction and the reliability of C_i decreases. The same holds for the arm region of the “Allegorie” dataset.

The globally operating graph labeling algorithm in general performs significantly better than the local path integration method. It also handles the few singletons at $N = 91$ well and propagates the correct phase over almost the full objects. In theory, the graph labeling method can also be applied without the candidate map. In this case, each label is available per pixel and the relative phase position is fixed by assigning a fixed label to some pixel(s). We tried this but memory consumption and processing time of this approach are unfeasible.

7 CONCLUSION

In this paper we proposed a general approach for using the epipolar geometry of multiple cameras in the context of phase unwrapping. We introduced the concept of the candidate map to aggregate all geometrically feasible unwrapping possibilities. In contrast to state of the art methods, we understand the candidate map as a preprocessing step, that can support *any* subsequent phase unwrapping algorithm.

The effect of the candidate map was illustrated by

augmenting two exemplary unwrapping methods: A local path following and a global minimum norm approach. Our results illustrate, that both algorithms greatly benefit from the additional constraints provided by our candidate map. This is particularly important for application domains that require fast acquisition speed and thus a low amount of captured images such as real time scanning. Robust, temporal unwrapping cannot be applied here. Together with the fact that additional cameras also relax the need for a gamma calibration we thus suggest to use at least two cameras for such a respective system.

ACKNOWLEDGEMENTS

The work presented in this paper has been partially funded by the project DENSITY (01IW12001).

REFERENCES

- Abdul-Rahman, H., Gdeisat, M., Burton, D., Lalor, M., Lilley, F., and Moore, C. (2007). Fast and Robust Three-Dimensional Best Path Phase Unwrapping Algorithm. *Applied Optics*, 46(26):6623–6635.
- Bergmann, D. (1995). New approach for automatic surface reconstruction with coded light. volume 2572.
- Bioucas-Dias, J. M. and Valado, G. (2007). Phase unwrap-

- ping via graph cuts. *IEEE Transactions on Image Processing*, 16(3):698–709.
- Boykov, Y., Veksler, O., and Zabih, R. (2001). Fast approximate energy minimization via graph cuts. *IEEE Trans. Pattern Anal. Mach. Intell.*, 23(11):1222–1239.
- Bräuer-Burchardt, C., Kühmstedt, P., and Notni, G. (2013). Phase unwrapping using geometric constraints for high-speed fringe projection based 3d measurements. volume 8789.
- Bräuer-Burchardt, C., Munkelt, C., Heinze, M., Kühmstedt, P., and Notni, G. (2008). Phase unwrapping in fringe projection systems using epipolar geometry. In Blanc-Talon, J., Bourennane, S., Philips, W., Popescu, D., and Scheunders, P., editors, *Advanced Concepts for Intelligent Vision Systems*, number 5259 in Lecture Notes in Computer Science, pages 422–432. Springer Berlin Heidelberg.
- Bräuer-Burchardt, C., Munkelt, C., Heinze, M., Kühmstedt, P., and Notni, G. (2011). Using geometric constraints to solve the point correspondence problem in fringe projection based 3d measuring systems. In Maino, G. and Foresti, G., editors, *Image Analysis and Processing ICIAP 2011*, volume 6979 of *Lecture Notes in Computer Science*, pages 265–274. Springer Berlin Heidelberg.
- Costantini, M. (1998). A novel phase unwrapping method based on network programming. *Geoscience and Remote Sensing, IEEE Transactions on*, 36(3):813–821.
- Dias, J. M. B. and Leito, J. M. N. (2002). The zm algorithm: a method for interferometric image reconstruction in sar/sas. *IEEE Transactions on Image Processing*, 11(4):408–422.
- Garcia, R. and Zakhor, A. (2012). Consistent stereo-assisted absolute phase unwrapping methods for structured light systems. *Selected Topics in Signal Processing, IEEE Journal of*, 6(5):411–424.
- Ghiglia, D. C. and Romero, L. A. (1996). Minimum Lp-norm two-dimensional phase unwrapping. *J. Opt. Soc. Am. A*, 13(10):1999–2013.
- Goldstein, R. M., Zebker, H. A., and Werner, C. L. (1988). Satellite radar interferometry: Two-dimensional phase unwrapping. *Radio Science*, 23(4):713–720.
- Gorthi, S. S. and Rastogi, P. (2010). Fringe projection techniques: whither we are? *Optics and Lasers in Engineering*, 48:133–140.
- Guo, H., He, H., and Chen, M. (2004). Gamma correction for digital fringe projection profilometry. *Appl. Opt.*, 43(14):2906–2914.
- Guo, H., Zhao, Z., and Chen, M. (2007). Efficient iterative algorithm for phase-shifting interferometry. *Optics and Lasers in Engineering*, 45(2):281–292.
- Han, X. and Huang, P. (2009). Combined stereovision and phase shifting method: a new approach for 3d shape measurement. volume 7389, pages 73893C–73893C–8.
- Hartley, R. I. and Zisserman, A. (2004). *Multiple View Geometry in Computer Vision*. Cambridge University Press, ISBN: 0521540518, second edition.
- Herráez, M. A., Burton, D. R., Lalor, M. J., and Gdeisat, M. A. (2002). Fast two-dimensional phase-unwrapping algorithm based on sorting by reliability following a noncontinuous path. *Applied Optics*, 41(35):7437–7444.
- Kolmogorov, V. and Zabih, R. (2004). What energy functions can be minimized via graph cuts? *Pattern Analysis and Machine Intelligence, IEEE Transactions on*, 26(2):147–159.
- Loffeld, O., Nies, H., Knedlik, S., and Wang, Y. (2008). Phase unwrapping for sar interferometry - a data fusion approach by kalman filtering. *IEEE T. Geoscience and Remote Sensing*, 46(1):47–58.
- Martinez-Espla, J. J., Martinez-Marn, T., and Lopez-Sanchez, J. M. (2009). A particle filter approach for insar phase filtering and unwrapping. *IEEE T. Geoscience and Remote Sensing*, 47(4):1197–1211.
- Peng, T. and Gupta, S. K. (2008). Algorithms for generating adaptive projection patterns for 3d shape measurement. *Journal of Computing and Information Science in Engineering*, 8(3):031009.
- Schlesinger, D. and Flach, B. (2006). Transforming an arbitrary minsum problem into a binary one. Technical Report TUD-FI06-01, Technische Universität Dresden.
- Wang, Z., Nguyen, D. A., and Barnes, J. C. (2010). Some practical considerations in fringe projection profilometry. *Optics and Lasers in Engineering*, 48(2):218 – 225. Fringe Projection Techniques.
- Xu, W. and Cumming, I. (1999). A region-growing algorithm for InSAR phase unwrapping. *IEEE Transactions on Geoscience and Remote Sensing*, 37(1):124–134.